X-Ray Spectral Variability of the Narrow-Line Seyfert 1 Galaxy NGC 4051 Observed with *Suzaku*

Manami Seino,[1] Hirofumi Noda,[2] Katsuma Miyake,[1] Kazuhiro Nakazawa[1] and Kazuo Makishima[3]

[1] The University of Tokyo, [2] Tohoku University, [3] RIKEN
E-mail(MS): seino@juno.phys.s.u-tokyo.ac.jp

Abstract

The narrow-line Seyfert 1 galaxy NGC 4051 was observed with *Suzaku* twice in 2008 November, with an interval of 2 weeks. It showed a high X-ray flux of $\sim 2 \times 10^{-11}$ erg cm^{-2} s^{-1} at 2–10 keV, which varied by a factor of 2 in less than 500 s. To study the source variation on time scales of ~ 500 s, we took the spectral difference between bright and faint phases in one observation. This difference spectrum was represented by a single power-law (PL) with photon index $\Gamma \sim 2.2$. However, a simultaneous fitting to the time-averaged and difference spectra failed if only adding a reflection component to the $\Gamma \sim 2.2$ PL. By adding another harder PL as in Seyfert 1 galaxies (e.g. Noda et al. 2013), the fit became successful. Furthermore, the difference spectrum between the two observations showed a clear hard excess component in addition to the $\Gamma \sim 2.2$ PL. The result suggests that the new PL flux also varied in 2 weeks, which indicates a source size of $60R_{\rm g} < R < 10^5 R_{\rm g}$.

Key words: galaxies: active — galaxies: individual (NGC 4051) — X-rays: galaxies

1. Introduction

The X-ray spectra of active galactic nuclei are considered to consist of a power-law (PL) component with photon index $\Gamma \sim 2$, which varies on a time scale of $\sim$ ks, and its reflection component with Fe-K line which varies in $\sim$ month (Fabian & Miniutti 2005). However, this common view has not been fully tested against the most up-to-date data. Actually, Noda et al. (2011; 2013; 2014) revealed that more than one primary components exist in Seyfert 1 galaxies (Sy1s).

In this work, we investigated if the same view can be applied to narrow-line Seyfert 1 galaxies (NLS1s), whose black holes (BHs) are less massive and Eddington ratios are higher than those of Sy1s. NGC 4051 is a near-by (redshift $z = 0.0024$; Brinkmann et al. 1995) NLS1, with BH mass of $\sim 1.7 \times 10^6 M_\odot$ (Denney et al. 2009). Being bright and highly variable, this is one of the best targets for our study.

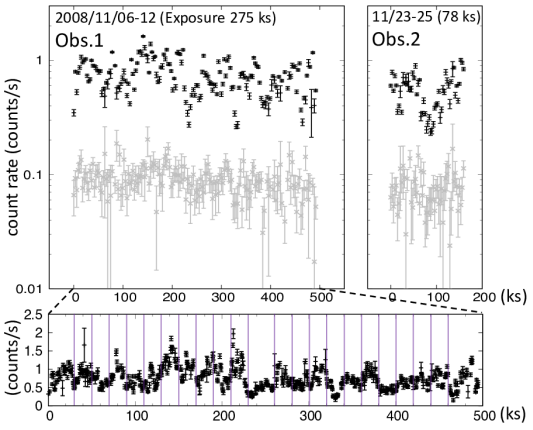

Fig. 1. Background-subtracted light curves of NGC 4051, obtained with XIS0+3 (2.0–10.0 keV in black) and HXD-PIN (15–45 keV in gray), shown with a binning of 3 ks. The lower panel shows the same XIS0+3 light curve in Obs.1 with 500 s binning, where vertical lines define data subsets.

2. Observation & Analysis

NGC 4051 was observed with *Suzaku* twice in 2008 November, with an interval of 2 weeks. We call the observations Obs.1 and 2 in chronological order (Fig.1) with exposures of 275 and 78 ks, respectivery. In the present work, we utilized data from the X-ray Imaging Spectrometer (XIS) and the Hard X-ray Detector with Si PIN photo-diodes (HXD-PIN). XIS events were extracted from a circular region of $3'.3$ radius centered on the source, and background events were from an annular region of the inner and outer radii of $5'.9$ and $8'.4$, respectively. The data of XIS0 and XIS3 (XIS0+3) using front-illuminated CCDs were added. We subtracted the HXD-PIN background provided by the HXD team, and modeled the Cosmic X-ray background based on Boldt

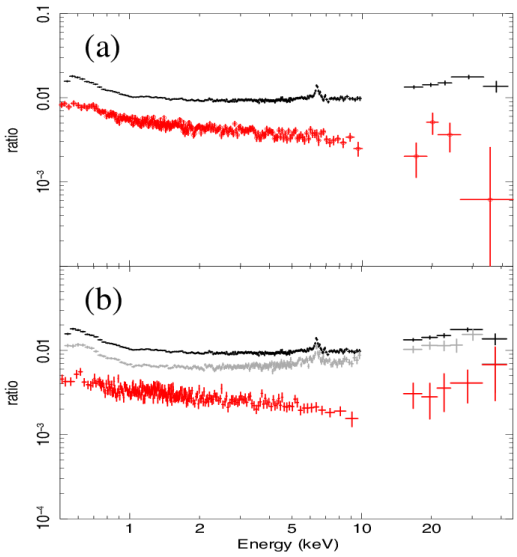

Fig. 2. (a)Time-averaged (black) and 500 s difference (red) spectra of NGC 4051 from Obs.1 obtained by XIS0+3 (2–10 keV) and PIN (15–45 keV). They are divided by a $\Gamma = 2.0$ PL. (b)Time-averaged spectra of Obs.1 (black) and Obs.2 (gray), and their difference (red).

(1987).

In Fig.2, we present time-averaged spectra of Obs.1 and 2, all divided by a prediction for a $\Gamma = 2.0$ PL. The spectral shapes of Obs.1 and Obs.2 are alike, and the intensity was 1.4 times higher in Obs.1 than in Obs.2. We divided the observation time of Obs.1 into 20–30 ks subsets (as shown in the lower panel of Fig.1), and made spectra of fainter and brighter periods than the average in each subset using the 500 s bin light curve. The red spectrum in Fig.2a is an overall difference spectrum, created by averaging 23 difference spectra from the individual subsets. It has a shape of $\Gamma \sim 2.2$ PL, and lacks the Fe-K line and the hard X-ray hump.

Then, we focus on the energy band above 2 keV

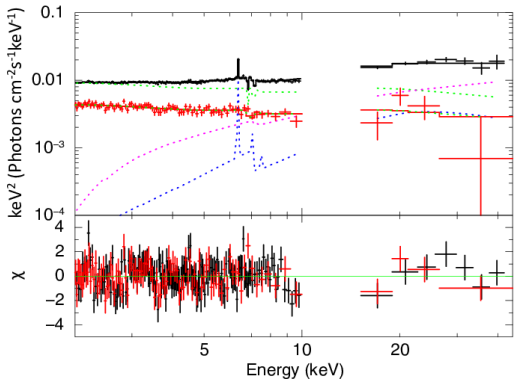

Fig. 3. Simultaneous fit to the time-averaged and 500 s difference spectra with the model described in text.

for model fitting. We simultaneously fitted the time-averaged and 500 s difference spectra of Obs.2. The difference spectrum was represented by a variable model (VM): $\mathrm{PL}_1 \times$ abs.(6.8 keV) $\times$ abs.(7.1 keV), and the time-averaged spectrum by the sum of VM′ and a stable model (SM). VM′ has the same fitting parameters as the VM except its normalization. We multiplied the whole model by galactic and ionized absorption.

First, we applied only a reflection component as SM, whose abundance and inclination angle were fixed at 1 solar and 60°, respectively. As a result, the difference spectrum was well explained by the VM, but some residuals remained in the time-averaged spectrum. Hence, we needed to add another component to SM. As this third component, we examined three candidates: another PL_2 with absorption, partial covering absorption of the variable PL_1, and relativistically smeared reflection of PL_1. As a result of fitting, independent PL_2 model best represented the spectra (χ^2/d.o.f $= 272/243$, partial covering: χ^2/d.o.f $= 296/244$, relativistic reflection: χ^2/d.o.f $= 292/244$). This component was a hard PL of $\Gamma = 1.5 \pm 0.3$ with equivalent hydrogen column density $N_{\mathrm{H}} = (5 \pm 4) \times 10^{22}$ cm^{-2} (Fig.3).

Furthermore, in the difference spectrum between the two observations, a hard X-ray hump in addition to the PL was seen (Fig.2b). Because there was no Fe K-line in the difference spectra, this hard X-ray hump can be said not to be the reflection component.

3. Discussion & Conclusion

The hard X-ray hump of the difference spectrum (Fig.2b) suggests the third component also varied in 2 weeks. From this time variability, we discuss the properties of the third component. If the hard PL is the right model, the time variability suggests that a size of the source is $60R_{\mathrm{g}} < R < 10^5 R_{\mathrm{g}}$. If partial covering, further fine tuning to explain both the spectral difference and time variability is needed. If relativistic reflection, we need a geometry to explain the 500 s invariability as well as the 2 weeks variability. Therefore, taking into account our model fitting in previous section, we conclude the hard PL emission is most reasonable.

References

Boldt, E. 1987, IAUS, 124, 611

Brinkmann, W. et al. 1995, A&AS, 109, 417

Denney, K. D. et al. 2009, ApJ, 702, 1353

Fabian & Miniutti 2005, arXiv:astro-ph/0507409

Miyake, K. et al. 2016, PASJ, 68, S28

Noda, H. et al. 2011, PASJ, 63, 449

Noda, H. et al. 2013, ApJ, 771, 100

Noda, H. et al. 2014, ApJ, 794, 2